SRI International

(2)

Quarterly Technical Report 4 • November 1992

FIELD-EMITTER ARRAYS FOR RF VACUUM MICROELECTRONICS

C.A. Spindt, Program Director
A. Rosengreen, Senior Research Engineer
P.R. Schwoebel, Research Engineer
Physical Electronics Laboratory

SRI Project 2743

Prepared for:

Defense Advanced Research Projects Agency
Defense Sciences Office
Virginia Square Plaza
3701 North Fairfax Drive
Arlington, VA 22203-1714

Attn: Dr. Bertram H. Hui

ARPA Order No. 8162

Contract MDA 972-91-C-0029

Covering the Period: 1 July through 30 September 1992

FIELD-EMITTER ARRAYS FOR RF VACUUM MICROELECTRONICS

C.A. Spindt, Program Director
A. Rosengreen, Senior Research Engineer
P.R. Schwoebel, Research Engineer
Physical Electronics Laboratory

SRI Project 2743

Prepared for:

Defense Advanced Research Projects Agency
Defense Sciences Office
Virginia Square Plaza
3701 North Fairfax Drive
Arlington, VA 22203-1714

Attn: Dr. Bertram H. Hui

ARPA Order No. 8162

Contract MDA 972-91-C-0029

Covering the Period: 1 July through 30 September 1992

APPROVED FOR PUBLIC RELEASE
DISTRIBUTION UNLIMITED

Approved:

Ivor Brodie, Director
Physical Electronics Laboratory

Donald L. Nielson, Vice President
Computing and Engineering Sciences Division

SRI International 333 Ravenswood Avenue • Menlo Park, CA 94025-3493 • (415) 326-6200 • FAX (415) 326-5512 • Telex 334486

REPORT DOCUMENTATION PAGE

Form Approved
OMB No. 0704-0188

1. AGENCY USE ONLY *(Leave Blank)*	2. REPORT DATE	3. REPORT TYPE AND DATES COVERED
	November 1992	Quarterly Technical 4 (1 July to 30 Sept. 1992)

4. TITLE AND SUBTITLE
Field-Emitter Arrays for RF Vacuum Microelectronics

5. FUNDING NUMBERS

6. AUTHOR(S)
C.A. Spindt, A. Rosengreen, and P.R. Schwoebel

7. PERFORMING ORGANIZATION NAME(S) AND ADDRESS(ES)
SRI International
333 Ravenswood Avenue
Menlo Park, CA 94025

8. PERFORMING ORGANIZATION REPORT NUMBER

9. SPONSORING/MONITORING AGENCY NAME(S) AND ADDRESS(ES)
Defense Advanced Research Projects Agency
Defense Sciences Office
Virginia Square Plaza
3701 North Fairfax Drive
Arlington, Virginia 22203-1714

10. SPONSORING/MONITORING AGENCY REPORT NUMBER

11. SUPPLEMENTARY NOTES

12a. DISTRIBUTION/AVAILABILITY STATEMENT
Approved for public release: distribution unlimited

12b. DISTRIBUTION CODE

13. ABSTRACT *(Maximum 200 words)*

SRI International has completed the fourth quarter of a program to develop field-emitter arrays for vacuum microelectronics. The goals of the effort are 5 mA at 5 A/cm2 for at least 2 hours, and demonstrated modulation of the emission at 1 GHz.

In-house technology was defined for the fabrication of low-frequency cathode structures on glass substrates. Fabrication and assembly of the apparatus required for microwave testing of the high-frequency cathode geometry was completed. Very-low-voltage cathode operation was demonstrated by fabricating cathode arrays using an experimental technique to produce gate apertures with 0.5-micrometer diameters. Current/voltage tests of high-frequency cathodes qualified them for testing in a microwave testing apparatus.

A field-emission microscope was fabricated and assembled for use in basic surface studies with the potential of developing cathode processing techniques that will maximize emission stability and uniformity over an array.

In bright light source research, 76,000 footlamberts was demonstrated with a standard P-53 phosphor and standard Spindt-type emitter array.

14. SUBJECT TERMS
Field-emitter array, vacuum microelectronics, low-capacitance cathode

15. NUMBER OF PAGES
38

16. PRICE CODE

17. SECURITY CLASSIFICATION OF REPORT	18. SECURITY CLASSIFICATION OF THIS PAGE	19. SECURITY CLASSIFICATION OF ABSTRACT	20. LIMITATION OF ABSTRACT
Unclassified	Unclassified	Unclassified	None

EXECUTIVE SUMMARY

SRI International has completed the fourth quarter of Phase I of a research and development program on the SRI Spindt-type field-emitter-array cathode with a view toward eventual applications in microwave amplifiers. Goals for this first phase have been set at 5 mA total emission, with a current density of 5 A/cm^2 for at least 2 hours and demonstrated modulation of the emission current at a frequency of 1 GHz. Our approach has been to identify methods of adapting and modifying the basic cathode structure of microwave operation and to experimentally investigate means of implementing those methods.

During the quarter we have accomplished the following, as documented in detail in this technical report:

- Continued research on basic cathode technology as defined by the goals of the DARPA program and related NRL project (Section 1)
- Established the in-house technology required to fabricate low-frequency cathode structures on glass substrates (Section 2)
- Completed the fabrication and assembly of the apparatus required for microwave testing of the high-frequency cathode geometry (Section 3)
- Demonstrated very-low-voltage cathode operation by fabricating cathode arrays using an experimental technique to produce gate apertures with 0.4-μm diameters (Section 3)
- Performed current/voltage tests of high-frequency cathodes, qualifying them for testing in the microwave testing apparatus (Section 4)
- Completed the fabrication and assembly of an emission microscope to be used in basic surface studies with the potential of developing cathode processing techniques that will maximize emission stability and uniformity over the array (Section 5)
- Demonstrated 76,000 foot-Lamberts with a standard P-53 phosphor and a standard Spindt-type emitter array (Section 6)
- Planned activities for the period of 1 October through 31 December (Section 7)

CONTENTS

ILLUSTRATIONS

1. INTRODUCTION

SRI International is participating in an effort of the Defense Advanced Research Projects Agency (DARPA) and the Naval Research Laboratory (NRL) to perform research and development on the SRI Spindt-type field-emitter-array cathode with a view toward eventual applications in microwave amplifiers. The current DARPA program is the vehicle for advancing the basic cathode technology for microwave applications (e.g., reducing intrinsic capacitance and driving voltage requirements), and continues the original program plan to establish the characteristics of the cathode in its preprogram state of development, identify methods of adapting and modifying the structure for microwave operation, and experimentally investigate means of implementing those methods. For the NRL program, which began earlier than the DARPA project, SRI has shifted emphasis to the support of NRL's in-house vacuum microelectronics program by providing NRL with state-of-the-art Spindt-type cathodes and consultation on setting up and using cathodes.

At the beginning of the program, two areas of development required immediate attention. The first was a materials and processing issue related to providing and maintaining a suitable vacuum environment for the cathodes. The second related to the cathode's inherent high capacitance and means for reducing that capacitance to a level that is consistent with the microwave applications envisioned for the cathode.

Our approach has been to research these two issues in parallel, using an easy-to-build, low-frequency-triode configuration fabricated on a TO-5 header as a test vehicle for materials and processing studies, and at the same time designing and researching fabrication techniques for building high-frequency-cathode structures on dielectric substrates (e.g., quartz or glass). Specific tasks that are being addressed on these related programs are:

1. Fabrication of a supply of state-of-the-art cathodes for use in establishing cathode characteristics, and for developing structures, circuits, and procedures for testing the cathodes as triodes
2. Development of a close-spaced anode test configuration that can be used to investigate triode characteristics at low frequency (kHz to MHz) in order to study the known problems with cathode survival under close-spaced anode conditions
3. Development of a circuit for driving the cathodes and demonstrating gain, frequency response, and peak emission levels
4. Studies of advanced cathode structures (geometry, fabrication technology, and processing) for high-frequency operation
5. Investigations (with NRL) of cathode mounting and connecting procedures using practices that are consistent with the microwave goals of the effort
6. Consultations with the NRL staff on the experimental results and applications of the cathode technology

2. LOW-CAPACITANCE CATHODE FABRICATION

The basic low-capacitance (LC) configuration is shown in Figure 1. The cathode consists of a single 1.25-mm-long line of emitter tips centered in a narrow overlapping area of the base and gate electrodes. The electrodes are designed to be 50-ohm microstrip lines with the substrate used. Four combinations of emitter tip pitch and overlapping width are being fabricated: (1) 5 μm pitch, 4 μm wide, (2) 5 μm pitch, 8 μm wide, (3) 2 μm pitch, 4 μm wide, and (4) 2 μm pitch, 8 μm wide.

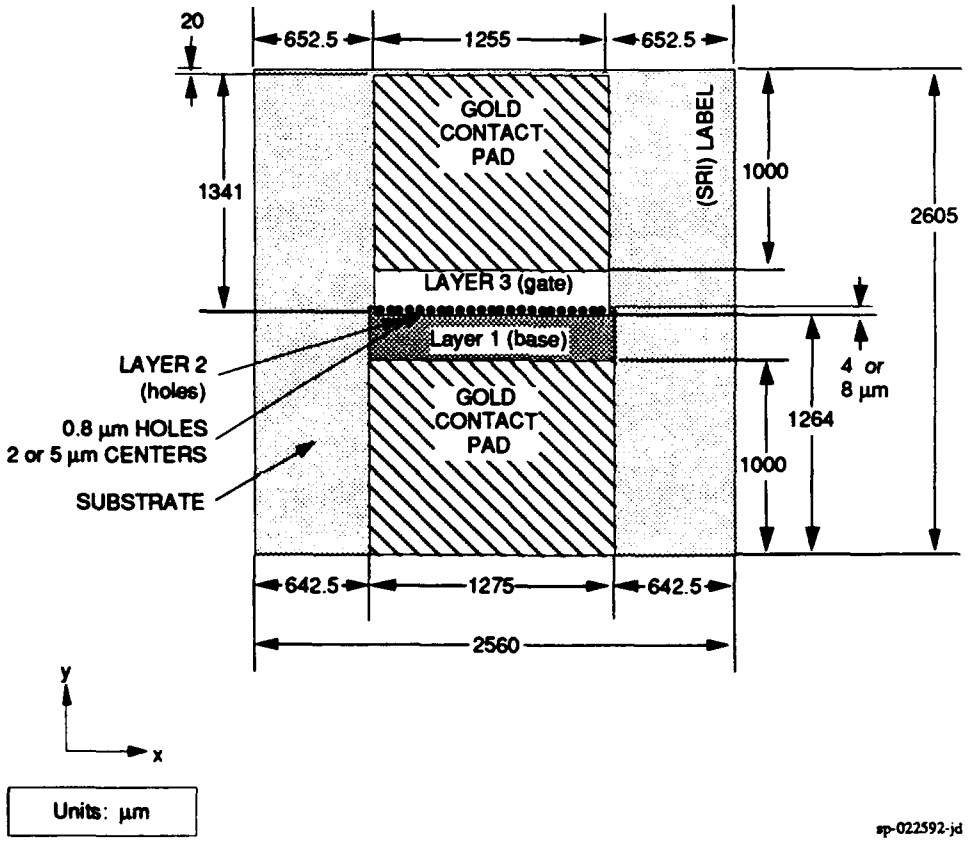

Figure 1. Detailed low-capacitance cathode layout

The task of transferring the basic cathode fabrication technology from silicon substrates to fused quartz or glass (Corning 7059) was completed. As the work continues, additional refinements will be made to the process, but we are now able to fabricate emitter arrays on glass substrates that have essentially the same operating characteristics as cathode arrays fabricated on silicon. In the course of developing the process, we brought several new tools and procedures on line. Most prominent of these are in-house plasma-enhanced chemical vapor deposition (PECVD) of a dielectric layer (SiO_2), reactive ion etching (RIE) of molybdenum and SiO_2, and

sputter deposition of metal and dielectric layers. In addition, we have established a close and beneficial working relationship with a foundry that services all of our high-resolution photolithographic requirements (0.8-μm-diameter hole patterns and registration to within 0.2 μm between layers). The fabrication process, as of the end of the reporting period, is as follows:

1. Vacuum deposit 1500 Å of Cr or Mo base film onto a 5-inch-diameter 7059 glass wafer.
2. Lithograph base pads in the base film (done with a stepper by our vendor).
3. Etch the base pads; RIE is used with the Mo base, and wet chemistry with the Cr.
4. Strip the photoresist and clean the wafer.
5. Deposit a SiO_2 insulating layer about 0.85 μm thick over the base pads using PECVD.
6. Deposit a Mo gate layer about 0.3 μm thick over the SiO_2.
7. Lithograph hole patterns in the gate film with a 5x stepper (done by our vendor).
8. Etch holes in the gate film and the oxide down to the base film.
9. Fabricate cones in the holes.
10. Pattern and etch (RIE) the gate electrode.
11. Pattern and etch away oxide from over the base electrode contact pad area.
12. Deposit Au contact pads ~2 μm thick on the base and gate contact pad areas.
13. Clean and mount for test or storage in vacuum.

There are several differences in the process described above and our standard cathode fabrication on silicon, and each of these differences required some measure of development in order to adapt it to the special needs of the field-emitter-array fabrication process. The most noteworthy of these are:

1. The base film was deposited with Cr rather than Mo for the first successful low-frequency cathodes, because we found that the wet chemistry available for patterning Mo lacked the required precision with respect to undercutting and uniformity along long edges. However, uniformity and a well-controlled undercut can be achieved with a standard commercial Cr etch. We have very recently developed an RIE etch for Mo, and this also produces a very well-defined edge with no undercut. As a result, we now can fabricate the base pad with either Mo or Cr. This flexibility may be useful in the future, and we will investigate fabricating both base and gate with Cr as well as making structures with Mo base and gate films. A disadvantage with the Cr is that it is attacked by phosphoric acid (H_3PO_4), and phosphoric acid has proven to be useful as part of the final clean-up processing of the cathodes prior to testing. On the other hand, Cr is much less susceptible to corrosion than is the Mo, and Cr also tends to adhere to other materials very well.

2. The oxide layer is deposited by PECVD in the low-capacitance configuration, whereas it is thermally grown in steam with the standard cathode configuration on silicon. Developing this in-house capability has been a significant advance in the flexibility available to us with our processing.

3. We have brought our RIE process on line for both Mo and SiO_2, and having this in-house capability is very important to the overall cathode fabrication process. RIE gives us more precise control over feature size in our structures than does wet chemistry because of the anisotropic nature of the RIE etch process.

4. Very precise mask alignment and etching procedures have been developed so that we are able to routinely produce 4-μm-wide strips, 1.25 mm long, with a row of emitter tips on 2-μm centers located in the middle of the strip along its entire length.

5. A process has been developed for depositing thick (~2 μm) Au contact pads on the cathode for lead bonding. This must be done after the cathode fabrication has been completed, and must not damage the emitters.

Figure 2 is a scanning electron micrograph (SEM) of a portion of a 1.25-μm-long linear array of 625 emitter tips made with the low-frequency cathode process. The gate apertures are about 1 μm in diameter, and the emitters are on 2-μm centers. The gate/base film overlap is 4 μm.

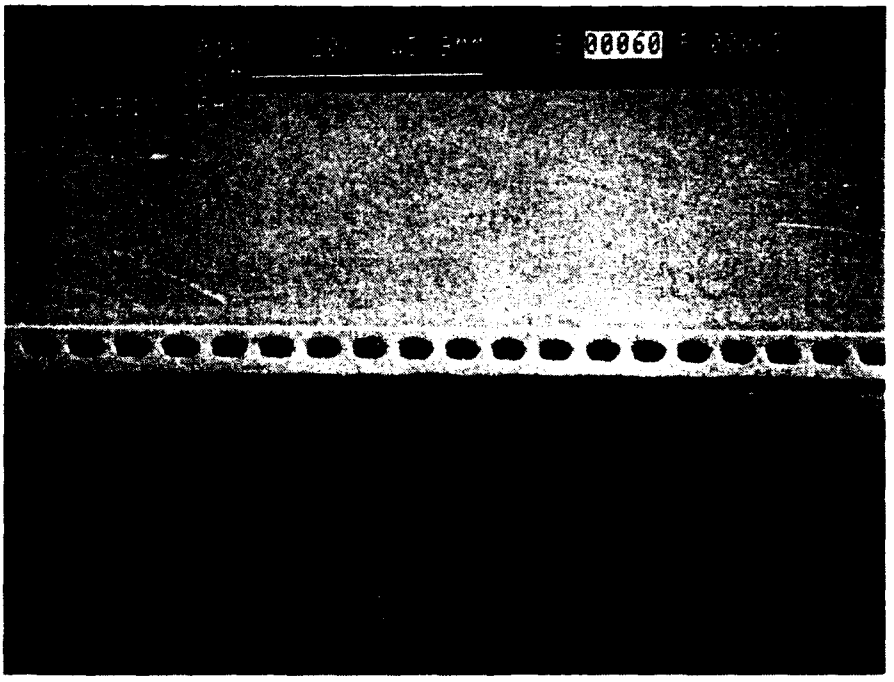

Figure 2. Scanning electron micrograph of a portion of a 625-tip array on 2-μm centers, with gate/base overlap 4 μm wide and 1.25 mm long

An additional reduction of the base-to-gate capacitance of the structure can be made by removing the SiO_2 from the active area (the area of overlap between the base and gate). This can be done by simply etching the oxide with hydrofluoric acid (HF). The dielectric constant of the insulating layer in the active area is then reduced from 3.8 to 1 with a proportional reduction in the capacitance of the overlapping portion of the structure. This may be significant at some point, and was shown to be possible. Figure 3 is a SEM of a structure fabricated in this way and then broken apart in an ultrasonic cleaner so that the interelectrode area is exposed. Note that the oxide has been completely removed from the interelectrode area.

Figure 3. High-magnification scanning electron micrograph of a portion of a 625-tip array on 2-μm centers with part of the gate film broken away ultrasonically to show removal of SiO_2 insulating film in the overlapping gate/base area

3. LOW-VOLTAGE CATHODE FABRICATION

It has been shown that reducing the dimensions of the Spindt-type cathode can significantly reduce the voltage required to produce a given emission. Reducing the voltage is important because it reduces the energy stored in the parasitic capacitance of the structure, and also helps to increase the transconductance of the device.

At the beginning of this program, the typical cathode geometry consisted of a 1.0- to 1.25-μm gate aperture diameter with the emitter tips centered in the aperture. As a result of experience gained with the stepper that is being used by our vendor, and by tailoring our etching processes to the task, we have been able to produce gate apertures with diameters in the 0.8-μm range with reasonable consistency. This reduction in size has been fruitful in that the voltage required for a given current has been reduced about 40% (1 mA at 130 V and 80 V, respectively, from 10,000-tip cathodes 52i-300-1L [0.8 μm] and 28C-279-7G [0.4 μm]). As near as could be measured with the SEM, all other geometric parameters were the same.

During the last reporting period, SRI entered into a self-funded cooperative program with an outside group (Siemens, Erlangen) that had a demonstrated capability to routinely produce gate apertures with diameters of 0.5 μm using photolithography and a proprietary process. Under this arrangement, the group would fabricate 100-hole arrays with the holes on 2.5-μm centers and diameters of 0.5 μm. We would then fabricate cones in the holes, perform tests, and share the resulting test data. No processing technology was to be shared. The group in fact delivered to us arrays with hole diameters of 0.4 μm. It was challenging to put cones in such small holes with an oxide thickness of about 0.6 μm, but an example of our success is shown in Figure 4, which is a SEM of a tip in a 0.4-μm-diameter gate aperture. Emission tests with these structures were very rewarding in that very low voltage produced very high currents. Figure 5 is a plot of the current/voltage^{-1} characteristics for a 100-tip array with 0.8-μm aperture diameters and a 100-tip array with 0.4-μm aperture diameters. Several important points can be made about the data shown in Figure 5. First, cathode 54C-304-5M with 0.8-μm apertures was operated up to 20 mA peak emission with a 60-Hz half-wave driving voltage. This is an average peak emission of 200 μA per tip for the 100 tips at a peak driving voltage of 173 V. By comparing the voltage required to produce 1 mA of emission from cathodes 54C-304-5M and 56C-S2-10L, we see 118 V and 59V, respectively. This is a 50% reduction in driving voltage achieved by reducing the aperture diameter from 0.8 μm to 0.4 μm.

The transconductance at the peak emission of 2 mA for cathode 56C-S2-10L is 3 μS per tip. Extrapolating to 20 mA, which was achieved with cathode 54C-304-5M, we see that 10 μS per tip should be possible. This would put the cutoff frequency (f_t) at about 10 GHz for the 625-tip low-capacitance cathode described in the previous section.

This small-diameter aperture work was done with SRI funds; however, the results could be very important to this program and are reported here for that reason. The effort triggered

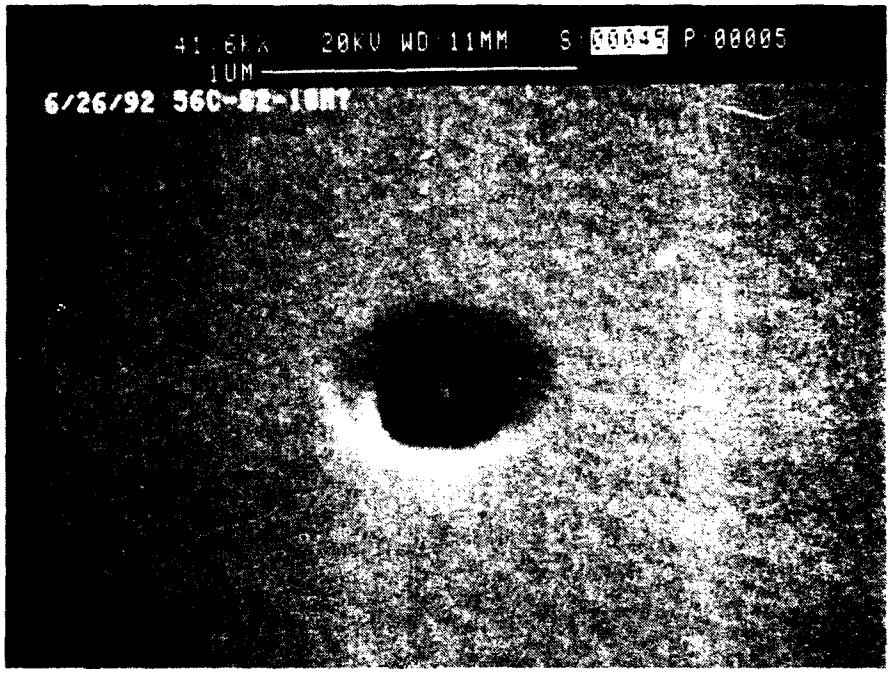

Figure 4. High-magnification scanning electron micrograph of an emitter tip in a 100-tip array with 2.5-μm center-to-center spacing

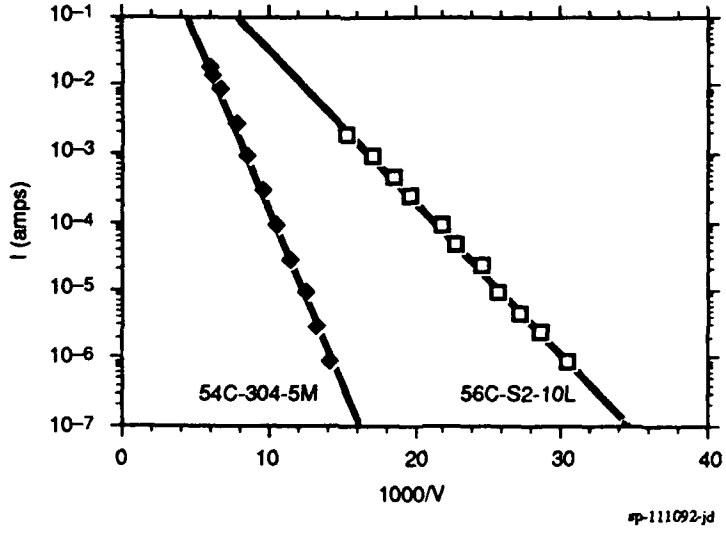

Figure 5. Current vs. 1/V for 100-tip cathodes 54C-304-5M (0.8 μm) and 56C-S2-10L (0.4 μm)

some SRI internal development work that has expanded on our base cathode technology and will therefore ultimately benefit this program.

Aperture diameters of less than 0.8 μm are not yet routine, but it has been clearly shown that they are possible, and very worthwhile developing.

The emitter tip work function is another very important parameter in determining the operating voltage for the cathodes. The work function is a materials and processing issue requiring careful surface studies. We will initiate surface investigations during the next quarter with the aid of a field-emission microscope (described in Section 5) that has been built in our laboratory for this purpose.

4. EMISSION TESTS

In addition to the low-voltage emission tests reported in the previous section, tests were conducted with the newly developed low-capacitance structures, and an emission life test that was initiated near the beginning of the program was continued.

4.1 LIFE TESTS

As of 30 September, a 1000-tip cathode (53i+300-7Q) has been operating continuously with a 60-Hz half-wave rectified drive voltage for a total of 10,224 hours, with the last 7,752 hours at 15 mA or higher peak emission. This is an average of 15 mA per tip with a peak drive voltage of 73 V. Figure 6 is a current/voltage oscillograph for this cathode. There has been no detectable change in the performance since the last quarterly report.

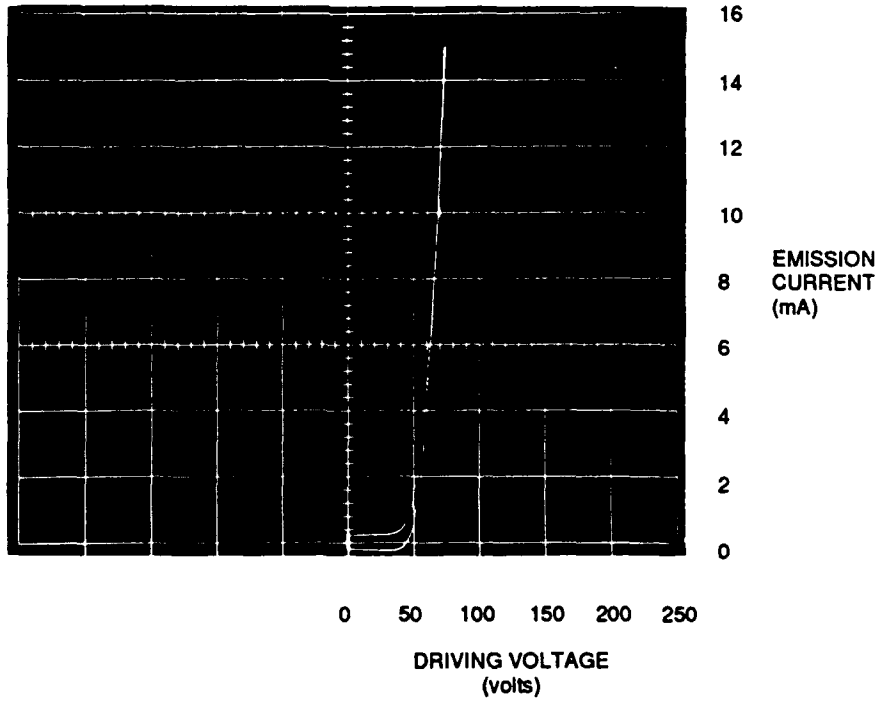

Figure 6. Current/voltage characteristics of cathode 53i+300-7Q (1000 tips) after 7,752 hours of operation at 15 mA peak emission with a 60-Hz half-wave driving voltage, with peak current density of 23 A/cm^2

4.2 LOW-CAPACITANCE CATHODE TESTS

Low-capacitance (LC) cathodes were tested in our standard test setup prior to being mounted in the new and unproven high-frequency (HF) apparatus described below. This was

necessary to qualify the low-capacitance structures, and assure that the several new process steps involved in their fabrication are compatible with the application. These tests were meant to give us a baseline on LC cathode performance so that we can reasonably evaluate the results we obtain with the HF setup. After tests in our standard setup with cathodes mounted in TO-5 headers, cathodes will be tested in our HF mounts with microstrip lines and SMA connectors for coupling to 50-ohm coaxial feedthroughs as shown in Figure 7. The first tests with the HF mounts will be done in a qualifying chamber having inexpensive low-frequency feedthroughs and in which six cathodes can be tested at a time. The purpose is to characterize the cathodes under conditions with which we are familiar prior to our dealing with microwave frequencies and the Hewlett-Packard network analyzer, which can introduce a host of complications. There are three important differences between the qualifying chamber and the HF test chamber shown in Figure 8: (1) the qualifying chamber has six test sites, whereas the HF test chamber has four, (2) the HF chamber has very expensive bakable SMA connectors and coaxial feedthroughs, whereas the qualifying chamber has relatively inexpensive low-frequency feedthroughs, and (3) the base and gate electrodes can be addressed independently in the qualifying chamber, whereas in the HF test chamber the base electrode is common with the ground plane. This means that gate-to-base current cannot be measured in the HF chamber, and gate-to-base current is an important indicator of a cathode's condition. Therefore, we considered it important to pretest the cathodes and their HF mounts in the qualifying chamber prior to placing the HF-mounted cathodes into the HF chamber. Performance in the HF mounts was evaluated against our previously established baseline.

When all is in place, the procedure will be to pretest and characterize six cathodes with HF mounts in the qualifying chamber while four are under test in the HF chamber and four others are being processed in a second, identical, HF chamber. Cathodes can then be cycled through the test systems as required.

4.3 LOW-CAPACITANCE CATHODE EMISSION TEST RESULTS

The first LC cathodes to successfully complete the newly established fabrication process described above were tested on TO-5 headers in our standard test setup at the end of the reporting period. Six cathodes were mounted in the system, and emission measurements were made with our standard 60-Hz half-wave driving voltage source. All six turned on and achieved at least 1 mA of emission. The highest level of emission was achieved with LC cathode 102L-E10-26B, which is a 625-tip array on 2-μm centers with an 8-μm-wide base-gate overlap. Figure 9 is an oscillograph showing the current/voltage characteristic for this cathode operating at a peak emission of 15 μA and a peak current density of 600 A/cm^2 at 143 V. The maximum emission obtainable in our standard test setup was limited by space charge effects between the gate and anode or collector. The standard test setup was designed to handle larger total currents, but is not well-suited for such large current densities.

Cathodes will be HF mounted and pumped out in the HF system at the beginning of the next reporting period.

(a) MICROWAVE TEST MOUNT

(b) CLOSE-UP OF CATHODE CHIP

Figure 7. Microwave test mount with microstrip lines and SMA connectors

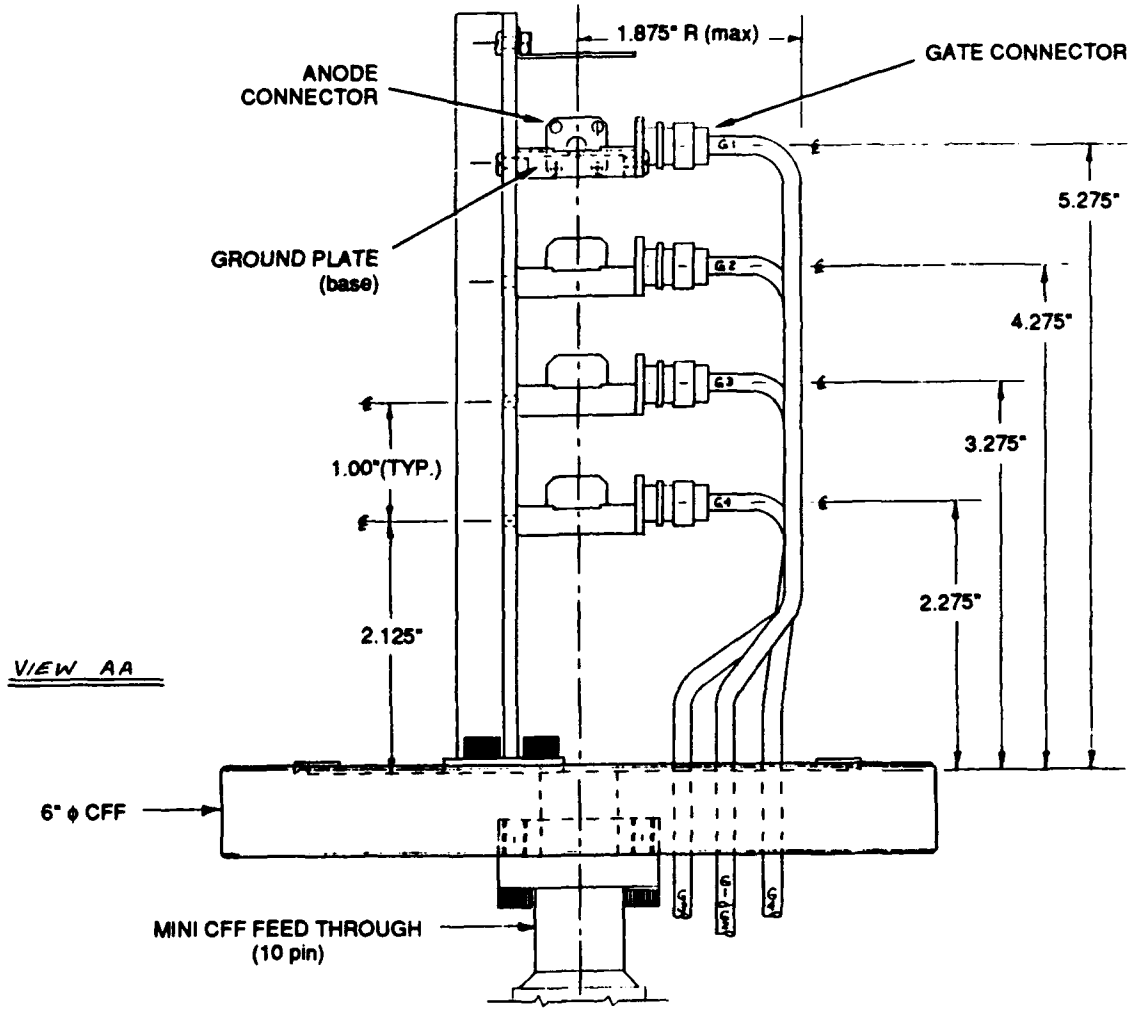

Figure 8. Layout of the high-frequency test apparatus with sites for four cathodes

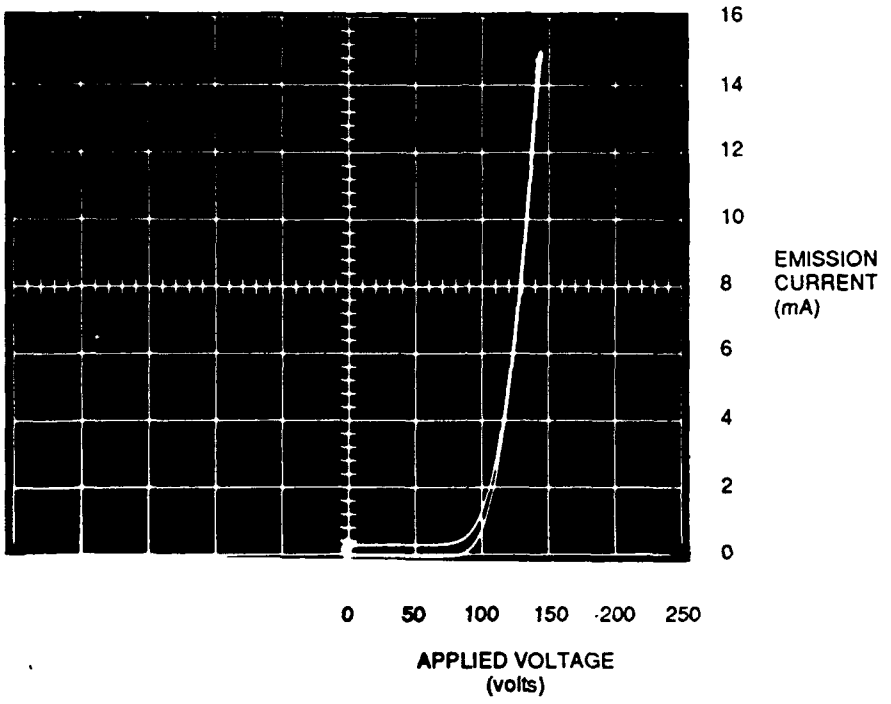

Figure 9. Current/voltage characteristics of low-capacitance cathode 102L-E10-26B at peak current density of 600 A/cm^2

5. FIELD-EMISSION MICROSCOPE STUDIES TO OPTIMIZE THE PERFORMANCE OF FIELD-EMITTER ARRAYS

Several important aspects are involved in the optimization of the performance of field-emitter arrays. Of primary importance is minimization of the required operating voltage and noise and maximization of the uniformity and stability of the electron emission. As the structural and chemical nature of the field-emitter surface govern the electron emission process, understanding and controlling the physical state of the surface is necessary if these goals are to be achieved in a systematic matter. To gather the necessary information, we have constructed a field-emission microscope (FEM) that, by allowing for direct imaging of the electron emission distribution at near atomic resolution and the simultaneous collection of current-voltage characteristics, facilitates understanding the effects of cleaning procedures, *in situ* processing, environment, operating parameters, coatings, and so forth on optimizing the performance of field-emitter arrays.

5.1 EXPERIMENTAL APPARATUS

The field-emission microscope we have constructed is based on a stainless-steel ultra-high-vacuum system and has a base pressure of $<3\times10^{-11}$ torr at room temperature. Figures 10 and 11 are photographs of the microscope and its associated control apparatus. Figure 12 is a schematic of the microscope vacuum chamber. The field-emitter array is mounted on a glass liquid-nitrogen cold finger having feedthroughs for the cathode operating voltage, cathode heater, and thermocouple. This allows for cathode operation and temperature control/measurement between 77 K and ~1300 K. The electron emission distribution is observed directly on the phosphor screen with an ~20-Å resolution of the emitter surface at a magnification of $\sim10^6$. The system is equipped with several ports that allow for additional electrical feedthroughs and the admission of various gases.

5.2 CATHODE PERFORMANCE OPTIMIZATION: EXPERIMENTAL APPROACH

The performance of the field-emitter array is governed by the Fowler-Nordheim [1928] equation

$$I = a(\beta V)^2 \exp(-b\phi^{3/2}/\beta V), \tag{1}$$

where I is the electron current, V is the applied voltage, ϕ is the work function of the emitter surface, and a and b, for practical purposes, can be considered constants. β is the field voltage proportionality factor defined by

$$F = \beta V, \tag{2}$$

Figure 10. Field-emission microscope and associated control electronics

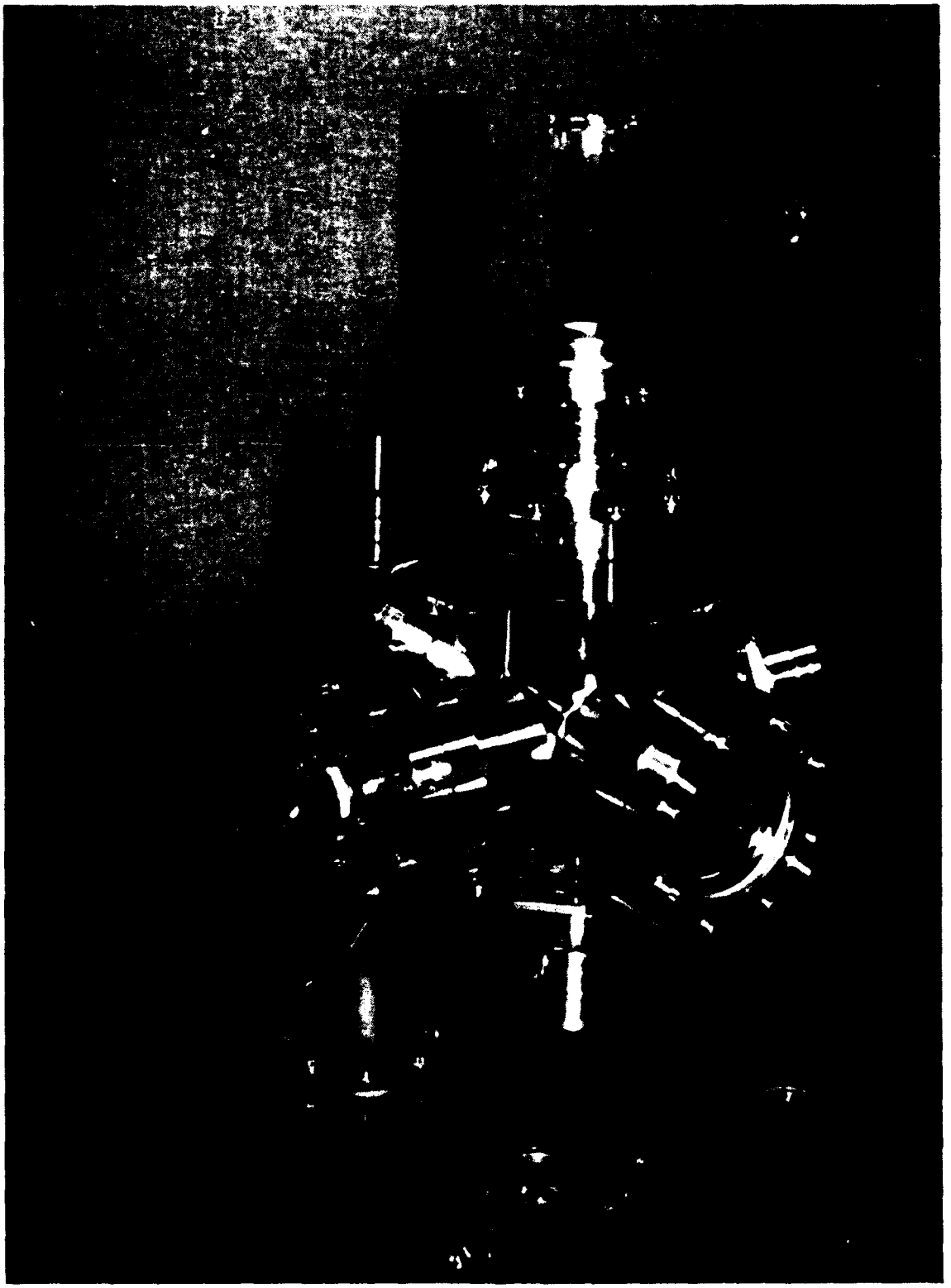

Figure 11. Close view of field-emission microscope

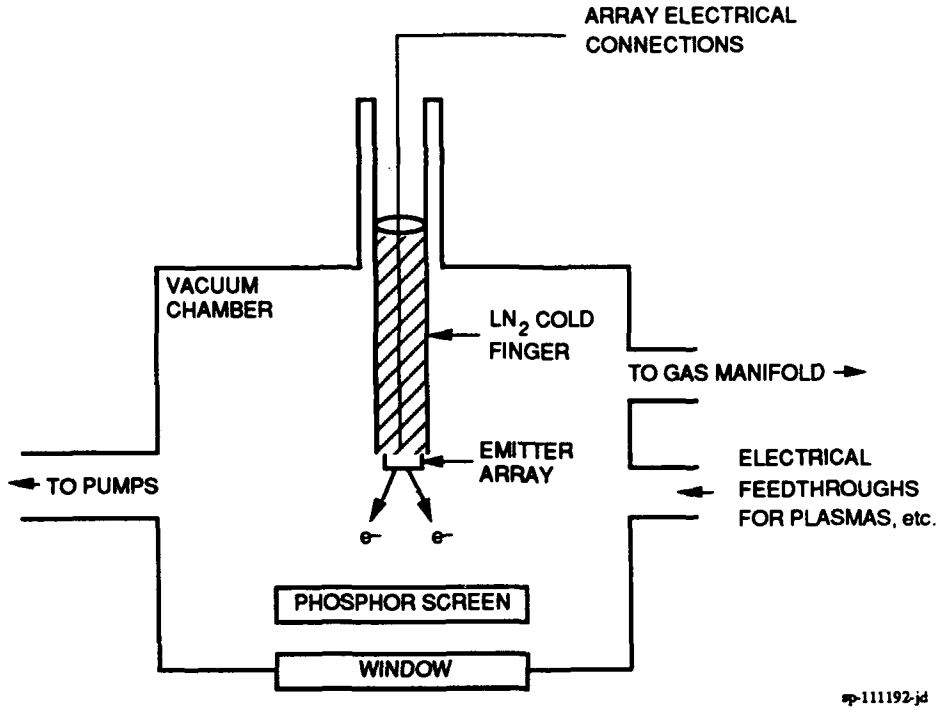

Figure 12. Schematic diagram of field-emission microscope, showing salient features

where F is the electric field at the emitter surface. The value of β is dependent on not only the macroscopic shape of the tip and its geometrical relationship with the anode, but also on the *microscopic* structure of the emitter tip surface in the high field region near the tip apex.

From Equation 1 we see that the emission current is a very sensitive function of β and ϕ. It is clear that the aspects involved in emission uniformity, stability, operating voltage, and noise depend on variations of β and ϕ with time.

With these basic physical principles in mind we have planned an experimental program that should systematically lead to the accomplishment of our goals concerning reliability. This program will follow a series of major investigations: (1) emitter tip array "cleaning," (2) *in situ* field-assisted enhancement of β, (3) vacuum coating of emitter tips, (4) background partial pressures studies, and (5) investigations of array emission uniformity. Initially, steps 1 through 4 will be performed on single microfabricated field-emitter tips so that the spatially overlapping emission distribution of many emitter tips is not viewed and measured. Following the experiments using single tips, where the physics is more readily interpretable, we will apply the same techniques to arrays of field emitters.

5.2.1 Emitter Tip Array Cleaning

If reproducible investigations are to be conducted, one must begin with a well-characterized emitter tip surface. Auger electron spectroscopy has shown that the majority of the surface contamination present on the emitter arrays is carbonaceous in nature—the result of organic contamination. With conventional field emitters, typically fabricated from etched,

polycrystalline refractory metal wire, high-temperature 'flashing' can be employed to desorb surface contaminants. However, as the temperatures required are near the melting point of the emitter tip material, such treatment cannot be employed to clean microfabricated field-emitter arrays because of the combination of a large difference in the melting points and thermal expansion coefficients of the materials utilized in their construction.

To circumvent these problems, we plan to investigate cleaning the arrays *in situ* using low-pressure plasmas. Previous research, involving the cleaning of large particle accelerator and fusion reactor vacuum chambers, has shown that hydrogen plasmas effectively remove carbonaceous contamination [Dylla, 1988]. We expect that such a procedure will result in more reliable initial emitter turn-on and increase both the uniformity and the long- and short-term stability of the emission current. We will first use single microfabricated tips, so that direct viewing of the emission distribution at near atomic resolution in the FEM, combined with current versus voltage and time measurements, will allow a determination to be made as to the optimum plasma treatment required. The results of these experiments can then be directly applied to the plasma treatment of large arrays.

5.2.2 *In Situ* Field-Assisted Enhancement of β

The second phase of experimentation will focus on investigating a 'forming process' that leads to a significant decrease (by up to a factor of ~4) in the operating voltage required to yield a given current. It has been observed in this laboratory that, under as yet somewhat unknown conditions, cathodes operating at elevated temperatures and high tip loading (current per tip) can exhibit a dramatic increase in their emission current at a given applied voltage [Brodie and Spindt, 1992]. Figure 13 shows Fowler-Nordheim data of an emitter array prior to and following such a change. It is likely that this process involves what is known as *thermal field buildup* [Bettler and Charbonnier, 1960].

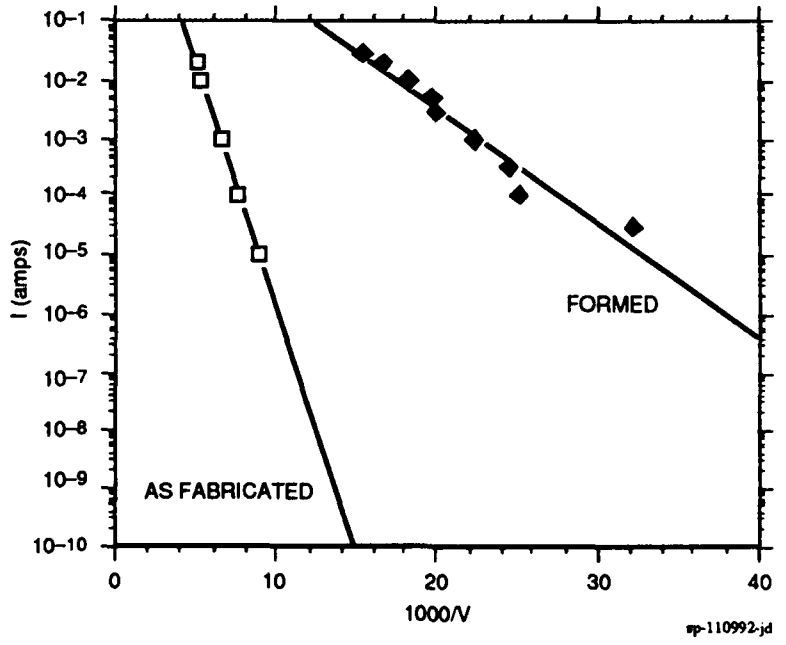

Figure 13. Current/voltage data for cathode 53i-300-23V prior to and following an enhancement of β

Thermal field buildup is electric field-assisted, thermally activated surface diffusion, and leads to the migration of surface atoms from the emitter shank to the apex. This results in a smaller effective tip radius and therefore a reduction in operating voltage for a given current. The equation governing the surface migration process is given by

$$F^2/8\pi = 2\gamma/r, \tag{3}$$

where γ is the surface tension coefficient, and r is the tip radius. This is simply a balance of the field energy, on the left, and the surface energy, on the right. One can see that if the field energy exceeds the surface energy, surface migration preferentially in the direction of the tip apex will occur, resulting in 'sharpening.' Similarly, if the surface energy exceeds the field energy, surface migration in the direction of the tip shank is preferred, resulting in tip blunting. From Equation 3 we can see that for $\gamma_{molybdenum} = 2100$ dynes/cm, electric fields on the order of 1 V/Å are required to reduce the tip radius to ~100 Å. Since the field emission current at 1 V/Å will be excessive, it may be necessary to reverse the polarity (emitter tip positive) to employ field forming for tip sharpening in the range of 100 Å.

We recall from Equation 1 that the voltage required for a given current is dependent on β, a geometrical factor related to the shape of the cathode and anode and their relative spatial relationship. One can show that β is directly proportional to the emitter tip radius; for a given electric field distribution at the emitter tip surface, halving the tip radius reduces the required operating voltage by a factor of 2.

By observing changes in the surface structure of the emitter tip and its current/voltage characteristics at controlled temperatures and applied fields in the field electron microscope, we should be able to determine the cause of a large increase in β. Once this process is understood and controlled it will be a very attractive means to perform final operational voltage reduction, *in situ.*

5.2.3 Vacuum Coating of Field Emitter Tips

These investigations will focus on the effects of various coatings on emitter tip operational characteristics with the primary goals of increasing long-term current stability and operational voltage reduction.

The guidelines to approaching coating technology as applied to emitter arrays can be deduced by again referring to Equation 1. The factors affecting current stability and operational voltage are controlled by β and ϕ. The effect of β on the operational voltage was discussed in the previous subsection. Here we are primarily concerned with changes in β and ϕ with time. These matters are of technological importance in applications where ideal vacuum conditions are not possible or practical to maintain.

Changes in ϕ are due to absorption/desorption phenomena of reactive, gas-phase species present as a result of vapor-pressure-driven outgassing or electron-stimulated desorption from surfaces bombarded during array operation. Changes in β are problematic only under more adverse conditions. For example, field-enhanced corrosion of the tip surface can occur in the region of the tip apex in the presence of water vapor. Here the formation and subsequent

desorption of metal oxide compounds leads to changes in the tip morphology (β) and therefore to changes in the current/voltage characteristics.

Unfortunately, it is very difficult to find a coating that will result in operational voltage reduction through decreasing ϕ, and yield high current stability. This is because low work function surfaces by definition are very chemically reactive. Thus, coatings must be tailored to the specific application.

For applications requiring operation in very poor vacuum environments a chemically inert coating is required, and one should expect little or no reduction in the operational voltage due to a decrease in ϕ. Here the previously discussed field forming of the emitter tips could be a viable means of voltage reduction, as it may be possible to sharpen the tip by applying a high field to the tip *during* the coating process. Polarization forces lead to preferential deposition of the coating material at the tip apex, possibly resulting in operational voltage reduction through a increase in β. Candidates to be investigated for such chemically inert coatings include carbon and various carbides.

For applications in which an ultra-high vacuum environment can be maintained, coating materials that will yield a low work function are of interest. Previous investigations in this laboratory have demonstrated, for example, that cesiated emitter arrays show improved characteristics (decreased voltage for a given current). However, other coatings, such as barium, are known to result in even lower work functions. Thus, further investigations will focus on the application of known low work function coatings to emitter arrays and studies of the resultant current/voltage characteristics, lifetime, and current stability.

5.2.4 Background Partial Pressures

The discussion regarding coating studies raises the subject of gas phase contamination and its influence on emitter array performance. As almost a subset of coating technology, testing the effects of gaseous contaminants on array current/voltage characteristics and stability will be necessary on an application-dependent basis. For example, in flat-panel technology, where pumping speeds are reduced, and ultra-high-vacuum-compatible materials may not be used in all construction materials, relatively high-background partial pressures of gas phase material will be present during operation. In such cases, mass spectrometry data can be used to identify the species present, and independent tests of their effects on operation can be made by intentional introduction in a controlled manner. In this way, problematic species can be identified, and construction processes or coating technology can be developed to eliminate any adverse effects on array performance.

5.2.5 Emitter Array Emission Uniformity

This series of investigations will culminate with studies of emission uniformity of emitter arrays. Our studies of array cleaning, voltage reduction, and vacuum coatings will be applied to arrays and then followed with studies of emission uniformity.

To conduct these investigations a simple einzel lens system will be installed in the emission microscope by which the electron emission from each tip in the array can be focused onto the phosphor screen and viewed (at a magnification of ~100 times) or measured at low

magnification with probe hole techniques. Measurements of the variation in the current/voltage characteristics from tip to tip will serve as a feedback mechanism through which our cleaning procedures, and so forth, may be adapted, if necessary, to maximize overall uniformity.

5.3 RESULTS

The field-emission microscope and basic control electronics have been constructed. Experiments to date with single, microfabricated field-emitter tips have focused on testing the overall operation of the vacuum system, electronics, and temperature control. The base pressure of the FEM has been found to be $< 3 \times 10^{-11}$ torr at room temperature, and emitter tip temperature control between 77 K and ~1000 K has been demonstrated. Other "shake-down" experiments on single tips have been conducted by observing long- and short-term current stability and measuring current/voltage characteristics at low temperatures.

The current/voltage characteristics of single, microfabricated molybdenum field-emitter tips were shown to be unaffected by operating temperatures between 77 K and 295 K. This result is to be expected in a very clean vacuum environment, as only the condensation of gas phase contaminants on the cooled emitter tip can modify ϕ and thereby the current/voltage characteristics.

Preliminary experiments have also been conducted on current stability with single field-emitter tips. With only relatively mild heating of the tip (and vacuum system) to ~250 °C for cleaning, we have observed that the current stability of single tips can be very high. Current fluctuations of <0.5% at total currents of 5 μA have been observed for several hours. Such quiescent periods can, however, be interrupted by periods of "burst noise," probably the result of the migration of surface contaminants to the emitting portion of the tip apex. Apparently, subsequent field desorption restores the initial current stability and current/voltage characteristics observed during the quiescent period. The plasma-cleaning procedure discussed in the previous subsection should eliminate the presence of such contaminants and with it the burst noise. The plasma-cleaning experiments are presently being initiated.

We believe that by the conclusion of the experimental program we have outlined, the combination of research into cleaning technique, voltage reduction, coatings, and emission uniformity should further enhance the spectrum of technological applicability for field-emitter arrays.

6. BRIGHT LIGHT SOURCE DEVELOPMENT

To obtain a high brightness from a phosphor, the current density must be high leading to degradation of the luminescent properties of the phosphor. Previous results indicated that a Wilemite phosphor may be recovered by an *in-situ* reoxidation employing a low-pressure oxygen gas discharge. This study was continued and the results are presented in the Appendix in the form of a paper submitted for publication. In this section we discuss the use of an yttrium-aluminum-garnet (YAG) based phosphor used in cathode-ray tubes for projection television.

The phosphors used in cathode-ray tubes are exposed to very high current densities to obtain the required high brightness, but worse than that, they are deposited on a glass surface that is not easily amenable to cooling. These phosphors must therefore be able to withstand high temperatures without significant degradation of their efficiency. Phosphors that are particularly well-suited for such a harsh treatment must be produced from very stable host materials such as YAG. In the experiments described here we used a very efficient green phosphor P53, $Y_3(AlGa)_5O_{12}$: Tb by Sylvania.

The phosphor screens were settled directly onto the anode from an aqueous suspension of phosphor and a potassium silicate binder. After deposition, the anode was baked in air at ~300 °C to dry the screen and set the binder. The method is similar to that employed in the television picture tube industry. The screen weight was maintained at ~5 mg/cm^2.

The light source is housed in an all-metal ultra-high-vacuum chamber operating in the 10^{-10} torr range. The experimental chamber is shown schematically in Figure 14. The field-emitter array is located ~2 cm away and at a 450° angle to the water-cooled, high-voltage anode. The phosphor layer is supported directly on the anode and can be raised to a voltage of 20 kV. The brightness of the phosphor is measured with a luminance probe through the viewing port opposite the phosphor sample. The control electronics allow for the measurement of brightness versus cathode duty cycles, electron current density, and electron accelerating voltage.

Because of the very high current densities and associated heating problems, the following results were obtained at pulsed operation. Figure 15 shows the brightness as a function of the duty cycle (10% duty cycle corresponds to a pulse repetition frequency [PRF] of 1 kHz) for two different electron currents. The pulse width and the anode voltage were 100 µs and 10 kV, respectively. The value of the anode voltage was limited by the vacuum feedthrough. At very low duty cycles the brightness curve is linear, but as the duty cycle increases saturation sets in. Nevertheless, it is possible to obtain a very high brightness as shown in Figure 16, where the current has been increased to 3 mA, resulting in a brightness of 76,000 foot-Lamberts at a duty cycle of 50%. At this level the screen was uncomfortably bright to watch. Figure 16 shows the brightness as a function of current at a duty cycle of 50%. At 3 mA the brightness has completely saturated. Assuming the light from the phosphor is in a narrow band close to 556 nm, where the eye has its maximum sensitivity, the luminous efficacy was calculated and plotted together with the brightness in Figure 17. At 3 mA, corresponding to ~15 mA/cm^2, the efficacy

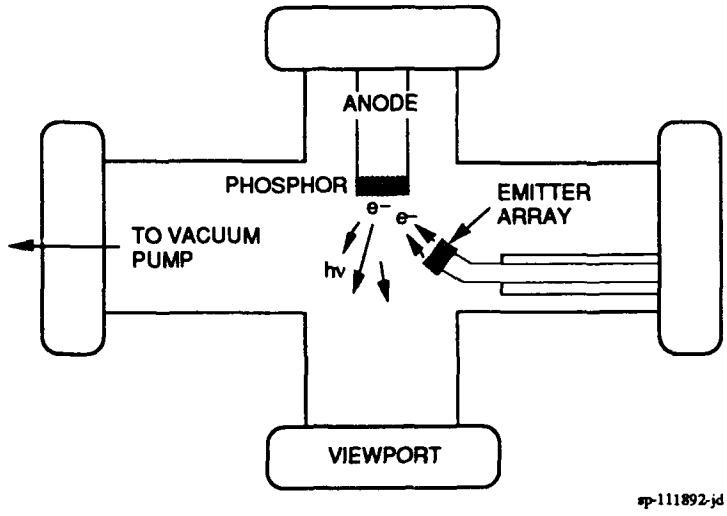

Figure 14. Light source test chamber

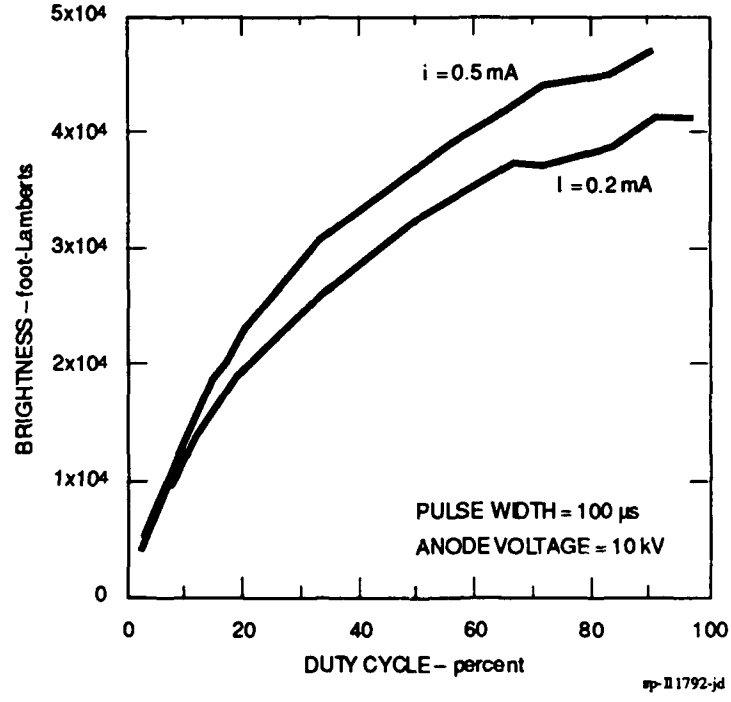

Figure 15. Brightness vs. duty cycle for electron currents of 0.5 mA and 0.2 mA

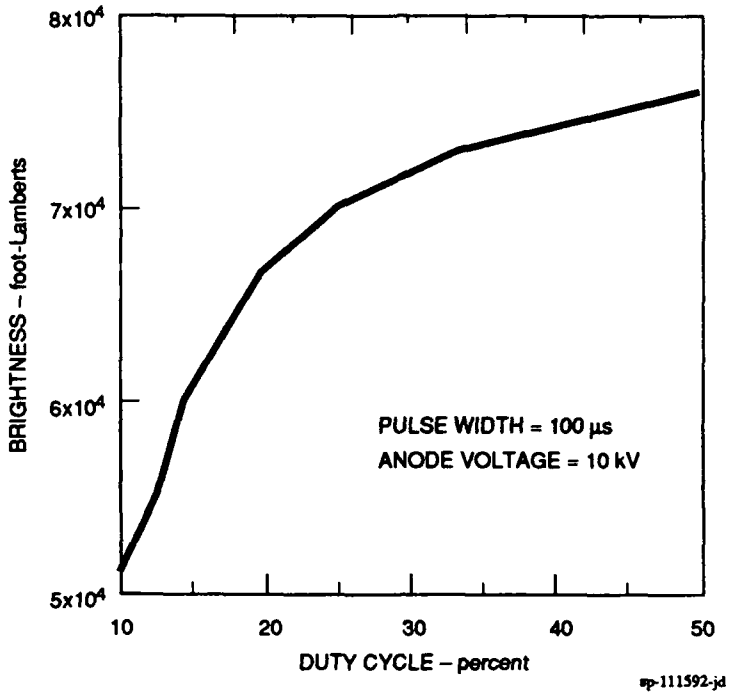

Figure 16. Brightness vs. duty cycle for electron currents of 3 mA

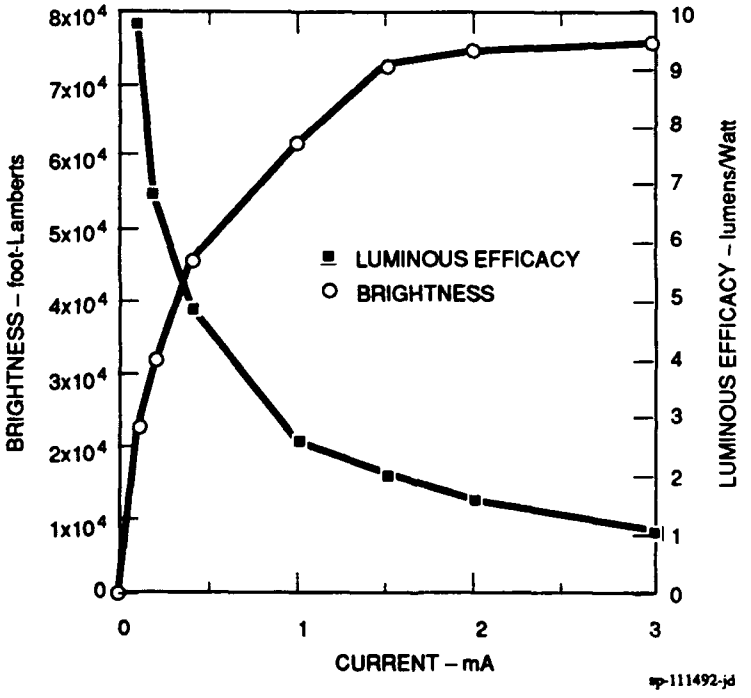

Figure 17. Brightness and luminous efficacy vs. current

has dropped by close to an order of magnitude from its low-current value. This indicates that although the metal substrate of the screen is water cooled, the phosphor grains make insufficient thermal contact with the substrate. Raue et al. [1989] report a luminous efficacy of 42 lumens/watt at low excitation densities and calculate an energy efficiency of 9%. If we use the value of 9.5 lumens/watt at 0.1 mA, this would correspond to an energy efficiency of 2%. They also report that the efficiency has dropped to half at an energy density of 70 mJ/cm^2. In our case this would correspond to a current of 14 mA. Clearly, improvements should be possible.

Our final experiment consisted of exciting the phosphor with pulses of constant energy but with variable pulse width at a PRF of 100 and 1000 Hz. The measured brightness is shown as a function of pulse width in Figure 18. The pulse energy was 2 mJ, corresponding to ~1 and 10 watts/cm^2 at 100 and 1000 Hz, respectively. The results show that the brightness decreases for pulse width below ~0.4 ms, although the number of electrons hitting the phosphor is constant. The reason for the drop is most likely thermal quenching. When the pulse width gets shorter than the thermal time constant involved in transferring the heat away from the phosphor, the temperature of the phosphor rises rapidly. If this is indeed the reason for the drop below 0.4 ms, the method for obtaining the results in Figure 18 would be a good way of getting information on the heat-conduction problem of the phosphor screen—information that is otherwise very difficult to obtain.

A quick literature search of the heat transfer problem of phosphors shows that this problem has been studied by others, including Vecht et al. [1992], who found that embedding metal strips of Mo and Ta in phosphors such as ZnS and CdS and diffusing the phosphor into the metal at temperatures in the range of 660 to 11000 °C did not destroy their luminescent properties. By the improved heat transfer provided by the metal, the researchers were able to use an anode voltage of 100 kV, resulting in a brightness in the range of 400,000 to 500,000 foot-Lamberts. Whether such a system would be practical and have a sufficient lifetime is not clear. Another approach, taken by Robertson and van Tol [1980] and Schmulovich [1989], is to produce YAG-based thin-film phosphors. These can be used at up to 10^4 watts/cm^2 and appear to have a long lifetime. For CRTs, trapping of light in the film may be a problem, but this should not be a problem in the lamp considered here because of the presence of a collection mirror.

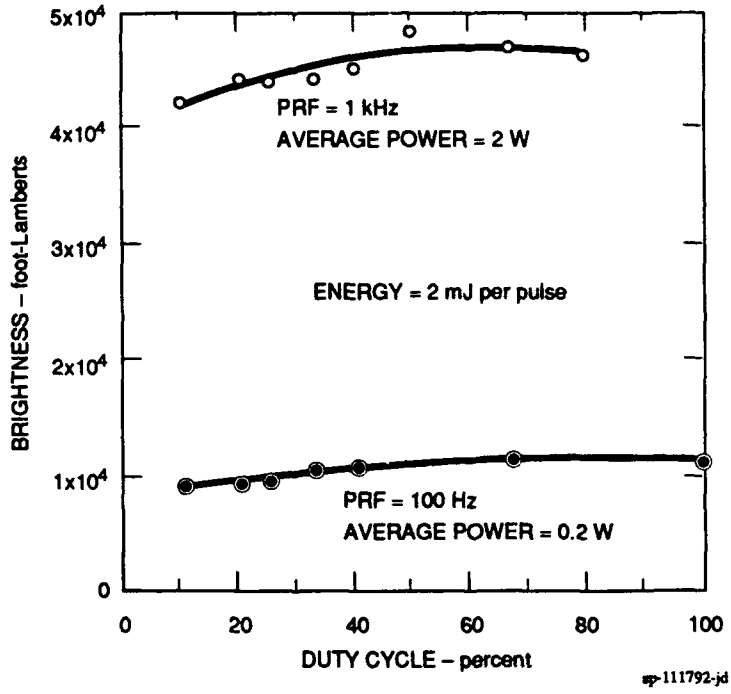

Figure 18. Brightness vs. pulse width for pulse excitation with pulses of constant energy at two different pulse repetition frequencies

7. WORK PLANNED

During the first part of the next quarter we will begin microwave frequency measurements on the cathodes with the Hewlett-Packard network analyzer. We will also continue development and fine tuning of the low-frequency cathode fabrication technology with a view toward improving yield, uniformity, and operating voltage.

Experiments with the field-emission microscope will begin with investigations of cathodes as fabricated to establish a baseline and will be followed by *in situ* processing experiments. These will include variations in temperature, pressure with selected gases, plasma processing, and the effects of adatoms on the emitter surfaces.

The phosphor experiments will continue with studies of methods for improving heat sinking of the phosphor and thin-film phosphors.

REFERENCES

Bettler, P.C., and F. M. Charbonnier, *Phys. Rev.*, **119**, 85 (1960).

Brodie, I., and C.A. Spindt, *Adv. Electronics and Electron. Phys.*, **83**, edited by P. W. Hawkes, Academic Press, NY (1992).

Dylla, H.F., *J. Vac. Sci. Technol.*, **A 6** (3), 1276 (1988).

Fowler, R.H., and L.W. Nordheim, *Proc. Roy. Soc. (London)*, **A 119**, 173 (1928).

Raue, R., A.T. Vink, and T. Welker, *Phillips Tech. Rev.*, **44** (11/12), 335-347 (1989).

Robertson, J.M., and M.W. van Tol, *Appl. Phys. Lett.*, **37** (5), 471-472 (1980).

Schmulovich, J., *Information Display*, **5** (3), 17-19 (1989).

Vecht, A., D.W. Smith, and G.P. Beyer, *SID 92 Digest*, 169-171 (1992).

APPENDIX

RECOVERY OF LUMINOUS EFFICIENCY OF DEGRADED WILLEMITE PHOSPHOR IN AN OXYGEN GLOW DISCHARGE

P. R. Schwoebel

Physical Electronics Laboratory

SRI International

Menlo Park, CA 94025

ABSTRACT

The luminous efficiency of Willemite phosphor is degraded by electron bombardment. Experiments are reported demonstrating that the luminous efficiency of the degraded phosphor can be recovered by exposure to a low-pressure oxygen glow discharge.

INTRODUCTION

The interest in obtaining high brightness from cathodoluminescent materials for cathode ray tube applications in, for example, projection TV and heads-up displays, has made phosphor degradation an important issue in tube lifetime.[1-3] The luminous efficiency decreases with time for a given input electron power. The decrease in efficiency can be directly correlated with the electron dose.[2,3]

Radiation damage leads to a decrease in the phosphor's luminous efficiency by mechanisms which appear to be material dependent. Klaassen *et al.* have reported an interesting study of how such radiation- induced phosphor degradation occurs in several cathodoluminescent materials.[4] In the case of Willemite (Zn_2SiO_4:Mn, designated P-1), a phosphor commonly used in heads-up display tube applications, Klaassen *et al.* [4] demonstrated that the degradation was caused by reduction of the Willemite surface by the electron bombardment. This oxygen-depleted surface layer was shown to result in a decreased luminous efficiency in agreement with a previous study of luminosity versus oxygen concentration at the Willemite crystal surface.[5] Heating of the crystals to 1100°C in pure oxygen for 3 hours increased the electron dose required to reach a given degradation level when compared to the electron dose required for unfired crystals.

Since aging processes relate directly to cathode ray tube life at high current densities, the possibility of *in situ* recovery of the luminous efficiency of the phosphor material offers an attractive means of extending operational lifetime. In a practical sense, this process must be compatible with the tube's construction, including the glass substrates upon which phosphors are often deposited.

As a means to recover luminous efficiency in Willemite phosphor *in situ* for tube applications, or to oxygenate other phosphors deposited on substrates that cannot withstand oxidizing atmospheres at high temperatures, phosphor oxidation in low-pressure oxygen glow discharges was investigated.

EXPERIMENTAL

The experiments were performed in an all-metal, ultra-high-vacuum chamber having a base pressure in the 10^{-10} Torr range. The electron source is a cold cathode field-emitter array[6] oriented at 45° with respect to the phosphor layer. The cathode is driven by a square-wave pulse generator with a pulse width of 20 μs, a duty cycle of 50%, and a voltage amplitude of ~ 125 to 175 V. The electron kinetic energy and current density at the phosphor surface were controlled with the positive high voltage applied to the anode; for these experiments the values were 10 keV and 0.5 mA/cm^2 (dc equivalent), respectively. The Willemite phosphor layer was settled onto a nickel-plated, water-cooled, copper, high-voltage anode. Potassium silicate was employed as the phosphor binder and the settled phosphor was baked at 300°C for 2 hours in air prior to installation in the vacuum system. A viewing port allowed for luminance measurements with a Tektronix model J6523 luminance probe.

Oxidation of the phosphor was conducted in a low-pressure (~10^{-3} Torr), pure oxygen (99.995%) dc glow discharge. The discharge electrodes were the vacuum chamber and the high voltage feed-through that supports the phosphor and were held at ground and negative potential, respectively. Thus the phosphor surface was bombarded by positive oxygen ions. To limit the current flow in the discharge, a 5 kΩ resistor was inserted between the power supply and the phosphor (cathode of the glow discharge). The average current density at the cathode was maintained at ~5 mA/cm^2 with a total glow discharge current of 10 mA and potential of 500 V.

RESULTS/DISCUSSION

The degradation of the as-prepared Willemite phosphor screen was monitored by measuring the brightness as a function of electron dose. A typical example of this characteristic is shown in Curve A of Figure 1. The initial rapid drop in brightness is often observed from Willemite.[2] Following such degradation, the phosphor was subjected to a low-pressure oxygen

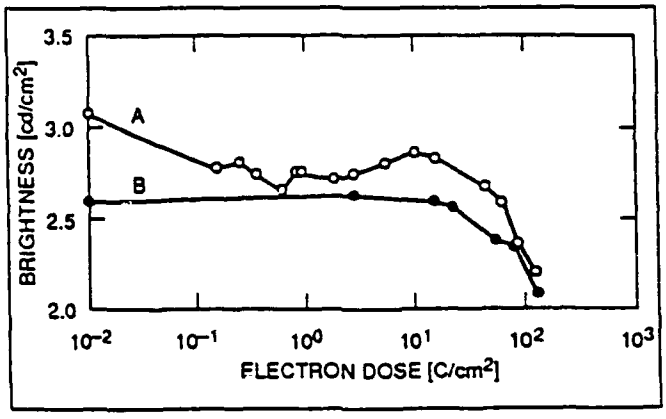

Figure 1. Brightness versus the electron dose for Willemite phosphor (electron energy 10 keV, electron current density 0.5 mA/cm^2). Curve A: Initial degradation of the Willemite. Curve B: Degradation of the Willemite used for Curve A following exposure to an oxygen plasma for 40 minutes (Plasma parameters: 500 V, total current 10 mA, current density ~5 mA/cm^2). The experimental error in these measurements is <1%.

plasma, *in situ*, as described above. For the experiment shown in Figure 1, the phosphor was subjected to the plasma for 40 minutes. After evacuation of the oxygen from the vacuum system, the degradation characteristics of the phosphor were again measured, with the results shown in Curve B of Figure 1. Note the increase in brightness over that of the lowest (final) level obtained during the initial degradation. Another consistent and interesting characteristic is the lack of the relatively rapid initial decrease in brightness with increasing electron dose observed with the undegraded Willemite.

Occasionally "bright-burn" is observed in the degradation characteristics of the plasma-treated phosphor. This refers to an initial increase in brightness of the phosphor with increasing electron dose prior to a decrease in brightness and is often observed during the initial degradation of Willemite.[7] Figure 2 shows an example of this behavior. Again, Curve A of Figure 2 shows the initial degradation characteristic of the phosphor; after plasma treatment for 4 minutes, the degradation characteristic shown in Curve B was obtained. Here, the brightness increases with increasing electron dose to a level that exceeds that shown in Curve A.

To examine the effect of plasma treatment time on recovery of luminous efficiency, degraded phosphors were subjected to relatively long exposures to the oxygen plasma. Exposure times on the order of 3 hours were found to cause further phosphor degradation to a level below that obtained initially. At the other extreme, plasma treatments of only a few seconds resulted in little or no observed improvement in the brightness of the degraded phosphor. Simply exposing degraded Willemite to an oxygen atmosphere at ~1×10^{-5} Torr at room temperature for several hours resulted in no improvement in the brightness.

Finally, preliminary experiments suggest that the percentage of improvement observed in luminous efficiency following oxygen plasma treatment increases with decreasing electron beam kinetic energy. The electron range decreases with energy, from ~5000Å at 10 keV in

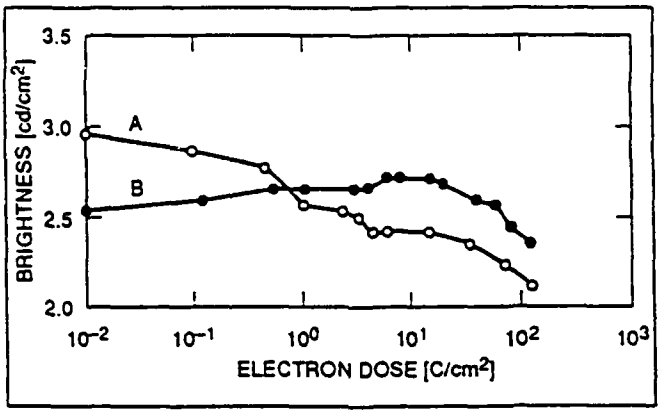

Figure 2. The brightness versus the electron dose for Willemite phosphor (electron energy 10 keV, electron current density 0.5 mA/cm^2). Curve A: Initial degradation of the Willemite. Curve B: Degradation of the Willemite used for Curve A following exposure to an oxygen plasma for 4 minutes (Plasma parameters: 500 V, total current 10 mA, current density ~5 mA/cm^2). The experimental error in these measurements is <1%.

Willemite,[8] indicating that the reoxidation in the glow discharge is most effective at the surface and near-surface region as may be expected.

CONCLUSIONS

These experimental results are consistent with the previously observed dependence of brightness on the oxygen concentration at the Willemite surface.[5] It is clear that an optimum oxidation time exists, given a set of glow discharge conditions, which will maximize the luminous efficiency of the degraded phosphor. The additional phosphor degradation observed upon extended exposure of the phosphor to the plasma may be due to a change in stoichiometry of the Willemite crystal surface region, possibly due to the presence of excess oxygen.

Future experiments will focus on understanding the fundamental processes involved in the degradation and recovery of the luminous efficiency in Willemite and other technologically important phosphors, with the goal of developing long-lived phosphorescent materials.

Discussions with I. Brodie and C.A. Spindt were very helpful during the course of this work. This research was supported by the Defense Advanced Research Projects Agency under Contract MDA972-91-C-0029.

REFERENCES

1. A. Martin, Adv. Electronics and Electron Phys. **67**, 183 (1986).
2. T. Hase, T. Tsuyoshi, E. Nakazawa, and H. Yamamoto, Adv. Electronics and Electron Phys. **79**, 271 (1990).
3. R. Raue, A.T. Vink, and T. Welker, Philips Tech. Rev. **44**, 335 (1989).
4. D. B. M. Klaassen, D.M. Leeuw, and T. Welker, J. Lumin. **37**, 21 (1987).
5. J.H. Hurd, Extended Abstracts of the ECS **74**, 220 (1974).
6. C.A. Spindt, C.E. Holland, A. Rosengreen, and I. Brodie, IEEE Trans. Electron Devices **38**, 2355 (1991).
7. H.W. Leverenz, Luminescence in Solids (Wiley, New York, 1950).
8. R.D. Evans, The Atomic Nucleus (McGraw-Hill, New York, 1955).